Time scales of circulation and mixing processes of San Francisco Bay waters

R. A. Walters[1], R. T. Cheng[2] & T. J. Conomos[2]
[1] *U.S. Geological Survey, 1201 Pacific Avenue, Tacoma, WA 98402, USA*
[2] *U.S. Geological Survey, 345 Middlefield Road, Menlo Park, CA 94025, USA*

Keywords: San Francisco Bay, circulation, estuaries, tidal currents, estuarine circulation, transport phenomena, mixing

Abstract

Conceptual models for tidal period and low-frequency variations in sea level, currents, and mixing processes in the northern and southern reaches of San Francisco Bay describe the contrasting characteristics and dissimilar processes and rates in these embayments: The northern reach is a partially mixed estuary whereas the southern reach (South Bay) is a tidally oscillating lagoon with density-driven exchanges with the northern reach.

The mixed semidiurnal tides are mixtures of progressive and standing waves. The relatively simple oscillations in South Bay are nearly standing waves, with energy propagating down the channels and dispersing into the broad shoal areas. The tides of the northern reach have the general properties of a progressive wave but are altered at the constriction of the embayments and gradually change in an upstream direction to a mixture of progressive and standing waves. The spring and neap variations of the tides are pronounced and cause fortnightly varying tidal currents that affect mixing and salinity stratification in the water column.

Wind stress on the water surface, freshwater inflow, and tidal currents interacting with the complex bay configuration are the major local forcing mechanisms creating low-frequency variations in sea level and currents. These local forcing mechanisms drive the residual flows which, with tidal diffusion, control the water-replacement rates in the estuary. In the northern reach, the longitudinal density gradient drives an estuarine circulation in the channels, and the spatial variation in tidal amplitude creates a tidally-driven residual circulation. In contrast, South Bay exhibits a balance between wind-driven circulation and tidally-driven residual circulation for most of the year. During winter, however, there can be sufficient density variations to drive multilayer (2 to 3) flows in the channel of South Bay.

Mixing models (that include both diffusive and dispersive processes) are based on time scales associated with salt variations at the boundaries and those associated with the local forcing mechanisms, while the spatial scales of variations are dependent upon the configuration of the embayments. In the northern reach, where the estuarine circulation is strong, the salt flux is carried by the mean advection of the mean salt field. Where large salinity gradients are present, the tidal correlation part of the salt flux is of the same order as the advective part. Our knowledge of mixing and exchange rates in South Bay is poor. As this embayment is nearly isohaline, the salt flux is dominated entirely by the mean advection of the mean salt field. During and after peaks in river discharge, water mixing becomes more dynamic, with a strong density-driven current creating a net exchange of both water mass and salt. These exchanges are stronger during neap tides.

Residence times of the water masses vary seasonally and differ between reaches. In the northern reach, residence times are on the order of days for high winter river discharge and of months for summer periods. The residence times for South Bay are fairly long (on the order of several months) during summer, and typically shorter (less than a month) during winter when density-driven exchanges occur.

Hydrobiologia 129, 13–36 (1985).

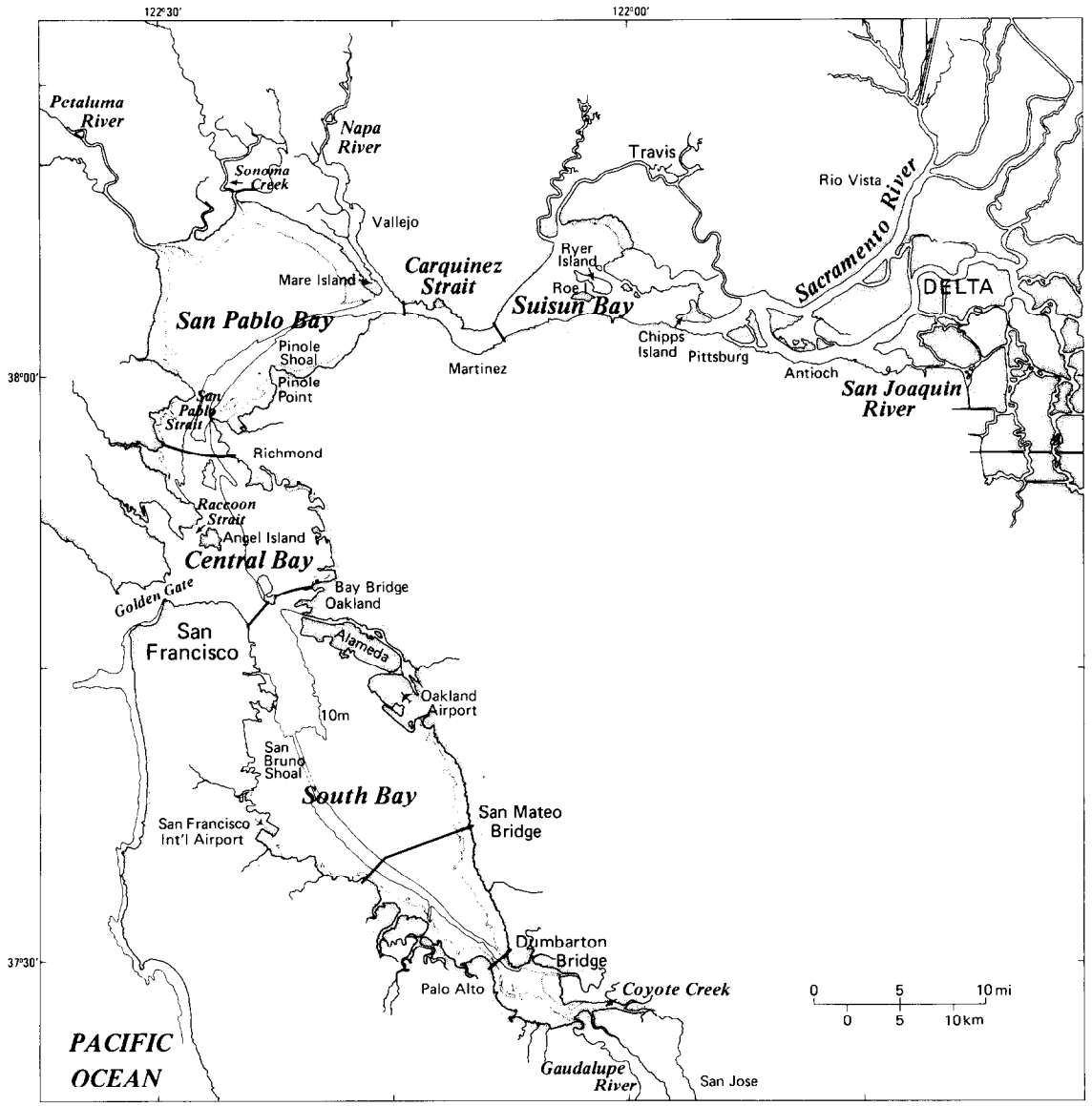

Fig. 1. The San Francisco Bay estuary. The northern reach includes Suisun Bay, San Pablo Bay, and the northern part of San Francisco Bay (to Golden Gate) whereas the southern reach is termed herein as South Bay.

Introduction

Our purpose in this paper is to provide a framework for the physical conditions and processes that exist in the San Francisco Bay estuary (Fig. 1). Such a framework provides at least a partial understanding of the types and importance of physical processes that control chemical and biological constituents. Circulation and mixing, the controlling physical processes in estuaries, are relatively complicated in San Francisco Bay because of the complex geometry and presence of several freshwater sources, and are not fully understood. We present a general conceptual understanding of the important physical process by partitioning them by time scale, then by partitioning the bay spatially into subregions.

Three basic time scales are defined as: (1) short-period variations (<1 h) associated with turbulence and small-scale motions; (2) tidal-period variations

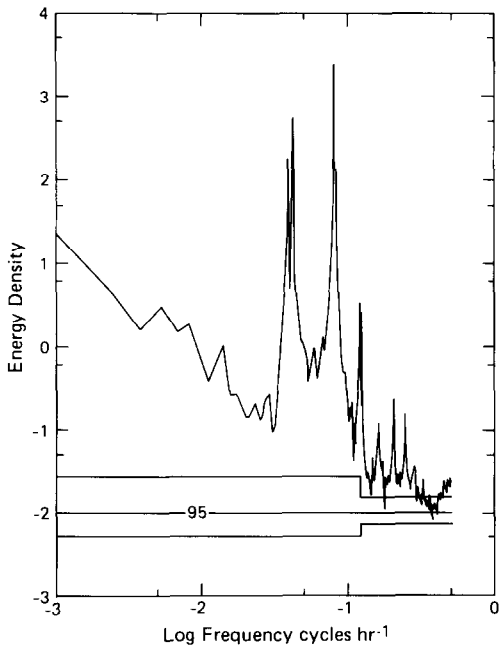

Fig. 2. Power spectrum for sea level at the San Mateo Bridge station (SMB). The two main peaks contain the diurnal and semi-diurnal tidal species; their harmonics are at higher frequencies. A 171-day data set of hourly values is used; smoothing is applied with a nonoverlapping box average with 6 degrees of freedom. The 95% confidence interval is shown on the bottom (after Walters, 1982).

(1–24 h) associated with tidal forcing and the generation of harmonics; and (3) long-period variations (>several days) associated with residual (nontidal) motions (Fig. 2). A consideration of short-period motions is beyond the scope of this paper. Rather, we will concentrate upon the tidal- and longer-period motions.

It is convenient to separate circulation into tidal and residual motions, but these are strictly separable only if they are linear processes, unlike the nonlinear characteristics of the bay. Thus, there are interactions among the tidal components of currents which give rise to low-frequency components (usually fortnightly and monthly) as well as direct interaction between the tidal period and low-frequency components. These interactions become particularly apparent in the discussion of residual currents. There is a strong spring-neap variation in most processes in the bay. This is a reflection of the fact that tidal energy is the dominant source for mixing and determines bottom stress in circulation. Because there is a strong spring-neap variability in the tides, there is a corresponding variability in the residual motions.

Before describing the spatial subdivisions of the bay, it is appropriate to consider the effects of the coastal ocean that are transmitted through Golden Gate (Fig. 1). The primary influences of the ocean and the bay are coastal variations in sea level due to tides, winds, and other meteorological influences, and variations in salinity and other water properties. At tidal time scales, sea level variations propagate into the bay as shallow water waves and can be quantified with the use of harmonic analysis and numerical tidal models. The long-period variations (3–5 d), due to events such as storms, have amplitudes of the order of 30 cm (Fig. 3). However, due to the long period, these variations appear as simultaneous (coherent) changes over the entire bay (it only takes 3–5 h for a wave to traverse the bay). Furthermore, because these changes are of such long period and small amplitude, they usually cause

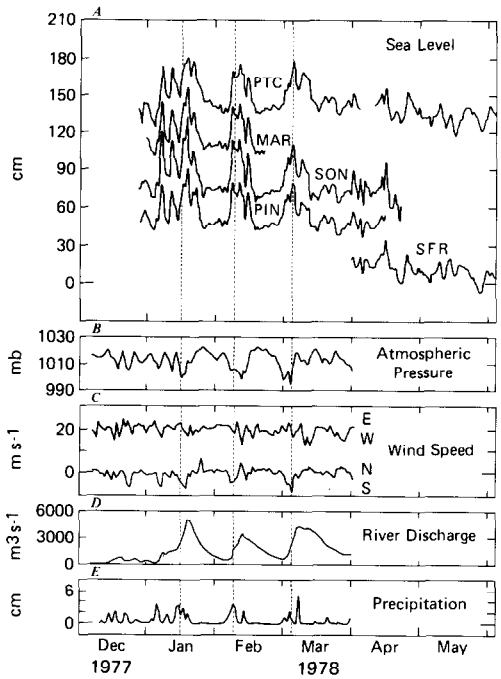

Fig. 3. (A) sea level (low-pass filtered), (B) atmospheric pressure, (C) wind speed, (D) Sacramento and San Joaquin River inflows, and (E) precipitation, San Francisco Bay, 1977–1978. Sea-level data from tide gauges at Port Chicago (PTC), Mare Island (MAR), Sonoma Creek Entrance (SON), Pt. Pinole (PIN), and Golden Gate (SFR), courtesy of National Oceanic and Atmospheric Administration. Atmospheric-pressure, wind-speed and precipitation data from San Francisco Airport.

insignificant effects in observed velocities (Walters, 1982). As a result, we need not consider these long-period variations in coastal sea level.

In addition, the salinity of the coastal water is relatively constant at about 34‰ with a seasonal variation of 1-2‰ (Churgin & Halminski, 1974). Variations of this magnitude are insufficient to cause significant variations in the strength of the estuarine circulation. However, in interpreting field data, one must be aware of seasonal oceanic variations in the various solutes as these reflect the source water concentrations.

There are two major spatial subdivisions with which we are concerned: (1) the northern reach and (2) South Bay. The northern reach has significant year-round freshwater input and is a partially-mixed to well-mixed estuary (Conomos, 1979). This reach, from Golden Gate to the confluence of the Sacramento and San Joaquin Rivers, is approximately 75 km long and includes three major embayments (Suisun, San Pablo and Central Bays) separated by constrictions at San Pablo and Carquinez Straits. Several dominant physical features are important in this discussion. A deep relict river channel that is deepest in the areas of constriction and most shoal in the center of San Pablo and Suisun Bays permits estuarine circulation to occur in the channel, whereas the more shoal areas act as controls upon the flow in that they inhibit the estuarine circulation. On the other hand, the wide embayments allow a large-scale horizontal flow and complicated mixing effects. Finally, the constrictions create high tidal velocities, increased turbulence, and enhanced vertical mixing. In this manner, they are also control points upon the flow.

South Bay can be characterized as a tidally-oscillating lagoon for most of the year (Conomos, 1979). In winter, however, it can have density driven exchanges with Central Bay. These exchanges result from two-layered circulation as in most estuaries, or from three-layered circulation similar to that in Baltimore Harbor (Cameron & Pritchard, 1963). Northern reach and South Bay are treated separately herein because the dominant physical processes in these two embayments are distinctly different from one another for most of the year.

Tidal period variations

Introduction

The water circulation in San Francisco Bay is primarily driven by the Pacific Ocean tides that propagate through the narrow opening at Golden Gate into the bay. For our purpose, 'tides' refers to sea-level variations, whereas 'tidal currents' is used to denote water movements. The water movements are strongly affected by the bathymetry of the embayment and are further affected by the earth's rotation and frictional resistance at the bottom of the basin. Salt-induced water stratification has only a minor role in the tidal period variations of the tides and tidal currents.

The ocean tides are generated primarily by the orbital motions of the moon around the earth and the earth around the sun (cf. Darwin, 1962) with the result that the primary tidal frequencies are clustered around the diurnal (24 h) and semidiurnal (12 h) period. Although the orbital motions of earth and moon are complex, the frequencies of these planetary motions can be determined very accurately (see the line spectra in Fig. 2). The effects of tide-generating forces are additive with each component of the tide-generating force producing one partial tide. There may also be several harmonics derived from nonlinear interactions between the partial tides. Locally, the water-level variations (tides) can be written as a sum of partial tides in which the frequencies of the partial tides are known. In practice, the local tidal amplitudes and phases are determined by fitting the water level data from long-term observations to the harmonic expression of the tides (Schureman, 1940). Once the amplitudes and phases of the major partial tides have been determined, they should remain invariant (if the external conditions which affect the tides at that location remain unchanged) and can be used for tidal predictions.

Conceptual model of tidal period variations in sea level and currents

Oceanic tides propagate landward through Golden Gate as shallow water waves and affect the entire estuarine system. The amplitudes and the phases of these incident tidal waves are modified by basin bathymetry, reflections of the waves from

shores, bottom friction, and by the rotational effects of the earth (Coriolis acceleration). Observations of the tides and tidal currents at Golden Gate were first described by Gilbert (1917) and Disney & Overshiner (1925). These observations and those reported by Cheng & Gartner (1984) have indicated that the tide is of mixed diurnal and semidiurnal type. There are two high waters and two low waters each day with the lower low water (LLW) following the higher high water (HHW). During the semidiurnal cycle, the ebbing current is usually stronger than the flooding. Following the lower low water is the lower high (LHW) water. The higher high water arrives roughly 50 min later each day.

Over time, the various partial tides become in-phase and out-of-phase with respect to each other, creating spring and neap tidal conditions on fortnightly and monthly time scales (see also Conomos *et al.*, 1985). During the spring tides, the partial tides reinforce each other such that the tidal height inequality is relatively large and the tidal currents are more intense. For neap periods the partial tides tend to cancel each other so that the tidal height inequality is relatively small and the strength of tidal currents becomes moderate.

The distinction between standing and progressive waves is central to understanding the major features of the tides and tidal currents in the bay. A progressive wave propagates down a long channel with wave crests moving forward at a certain phase speed that is a function of wave period and water depth. For tidal waves (shallow-water waves), the phase speed depends only upon the depth. The maximum forward current speed occurs at the crest of the wave and an oppositely directed current occurs at the trough. The horizontal current speed is zero at mean water level.

Standing waves typically occur in semi-enclosed basins where the wave is reflected back upon itself (for instance, standing waves on the windward side of a fixed object). Slack currents occur at high and low water and the water level oscillates up and down from crest to trough with no apparent propagation. In the bay system, the northern reach is characterized by having a partial progressive and standing wave, whereas South Bay is characterized by having a standing wave.

Another useful tool for understanding the tides is to compare the change in amplitude and phase along the bay axis, with respect to the reference

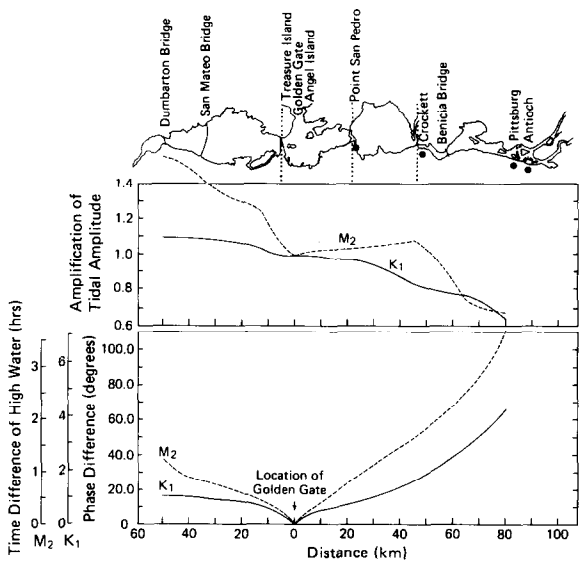

Fig. 4. Amplification of tidal amplitude (A) and shift of tidal phase (B) for M_2 partial tide and for K_1 partial tide. The amplitudes and phases are referenced to those at Golden Gate.

station at Golden Gate, as a function of distance from Golden Gate along the channels (Fig. 4).

The tide at Golden Gate is a mixture of a progressive and a standing wave. As the wave traverses Central Bay, the nature of the wave changes between the northern and southern shores due to the influence of the bathymetry of the embayments. The difference, noted in tide tables (National Oceanic and Atmospheric Administration, 1979), is striking. On the southern shore, the wave becomes more of a standing wave and the currents lead those at Golden Gate. Along the northern shore, the progressive nature of the wave remains and the currents lag those at Golden Gate.

Because South Bay is an enclosed embayment, the wave reflections from the south end of the bay are superimposed upon the incoming tides from Central Bay, and the tides become nearly standing waves. The phase lag of sea level increases slowly with distance away from Central Bay (Fig. 4). Near the south end of South Bay, the tidal currents precede the water levels by 2.5–3.0 h or nearly 1/4 of a tidal cycle, the characteristic of a standing wave (slack currents at high and low water).

A typical amplitude distribution for the semidiurnal tidal component (M_2) and the diurnal component (K_1) (Fig. 4) shows both amplification and dissipation. Both tidal components have longer pe-

riods than the resonance period for South Bay (about 7 h). However, the semidiurnal component is closer to resonance and hence has a much greater amplification than the diurnal component (Fig. 4). As the tidal wave propagates into South Bay, it is not entirely a standing wave due to bottom friction. As a result, the phase speed is higher in the deep channels than in the shoals. Hence, there is a tendency for the wave to propagate down the channels and then disperse into the shoals.

The tides in the northern reach are quite different and much more complex than in South Bay. As the tides propagate up the reach from Central Bay along the main channel, they maintain the general properties of a progressive wave (maximum current speed near high water). At the constrictions, however, the waves are partially reflected and superimposed on the tides in the main channel whose characteristics have gradually changed from mostly progressive waves to a mixture of progressive and standing waves. The wave amplitude increases up to the eastern shore of San Pablo Bay due to wave reflection (Fig. 4). Through Carquinez Strait, the tidal wave is highly attenuated by dissipation, and the amplitudes diminish.

Spatial variability of tidal currents

Bottom friction strongly affects the speed of the currents. The directions of the tidal currents are generally tangent to the basin isobaths, whereas the magnitudes of the tidal currents are proportional to the mean water depth. These properties are particularly evident in the transition regions between the main channel and the shoals. The root-mean-square (RMS) speeds are found to correlate linearly with the mean water depth for both South Bay (Fig. 5) and the northern reach (Cheng & Gartner, 1984, 1985). The ratio of the sum of tidal amplitude in diurnal tides over the sum of amplitude in semidiurnal tides is in the range of 0.25 to 0.60 suggesting that the tidal current is of mixed semidiurnal and diurnal type but inclining strongly towards the semidiurnal type. Since the M_2 tide is the largest semidiurnal component in the bay, it is probably also the most representative tidal current component.

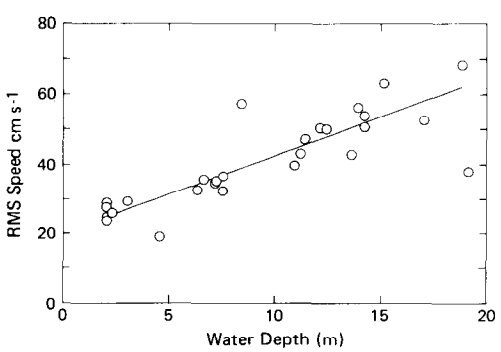

Fig. 5. Relationship between RMS current speed and water depth (MLLW) at deployment sites in South Bay.

The spring and neap variations of the tidal currents are very pronounced. The maximum tidal current speed at spring tides is estimated by $(M_2 + S_2) + (K_1 + O_1)$, where the symbols are the tidal current amplitudes of the respective partial tidal currents deduced from harmonic analysis (see Table 1). The maximum current speed at neap tides is estimated to be not less than $(M_2 - S_2) - (K_1 - O_1)$. The RMS tidal-current speeds have been calculated from available current data (Cheng & Gartner, 1984, 1985).

The spatial distributions of the properties of tidal currents are summarized in terms of the maximum speed of the M_2 (lunar semidiurnal) constituent, the estimated spring and neap currents, and the RMS speed (Fig. 6). These parameters are plotted in the principal current direction and depicted in the plan view.

Tidal excursion

Tidal excursion is the distance traveled by a water parcel within a tidal cycle. A progressive vector diagram can be constructed from current meter data as an estimate of tidal excursion (Cheng & Gartner, 1984). The estimated tidal excursion, however, is only an approximation because Eulerian data (from current meters) are used to represent a Lagrangian process. The mean tidal excursion can also be estimated from the RMS current speed times the half tidal period (in the principal tidal current direction). The dependence of the RMS speed on mean water depth (Fig. 5) implies that the tidal excursion is also a function of the local water depth. For an RMS speed of 60 cm s^{-1} (representing the water movements in the main channel), the mean tidal excursion is estimated to be about 13 km, whereas for an RMS speed of 35 cm s^{-1}

Table 1. Major partial tide and tidal current constituents in San Francisco Bay. Data from Cheng & Gartner, 1984.

Tidal Current		Golden Gate (C-1)			San Pablo Strait (C-18)			Suisun Bay (C237)			South Bay (C-9)		
	cycles d^{-1}	Major	Direction	Phase	Major	Direction	Phase	Major	Direction	Phase	Major	Direction	Phase
O_1	0.9295	18.4	80.0	36.7	18.6	17.3	37.4	12.8	102.0	82.0	6.6	167.4	31.5
K_1	1.0027	22.2	83.7	48.1	30.0	15.7	37.1	22.3	99.8	77.3	15.9	169.2	36.4
N_2	1.8960	24.8	69.5	262.2	14.6	17.8	279.7	19.2	99.4	356.7	7.0	166.6	275.5
M_2	1.9323	106.0	74.0	289.1	97.2	21.1	318.8	70.2	99.8	25.4	45.1	165.6	289.1
S_2	2.0000	28.9	72.1	287.1	24.5	22.8	308.4	27.7	97.3	13.0	7.7	164.1	190.3
M_4	3.8646	10.0	25.8	276.7	4.2	46.5	92.1	4.7	109.1	305.3	2.3	197.4	151.6
Water Level		Amplitude	Phase		Amplitude	Phase		Amplitude	Phase		Amplitude	Phase	
O_1	0.9295	22.9	97.2		21.1	109.2		16.3	145.0		23.1	107.8	
K_1	1.0027	36.7	106.4		35.1	119.8		28.3	150.5		38.9	116.1	
N_2	1.8960	12.4	317.3		12.2	343.1		8.8	32.0		15.4	339.8	
M_2	1.9323	57.8	337.8		59.1	3.6		48.9	53.3		75.2	357.3	
S_2	2.0000	13.5	336.6		13.5	1.9		10.1	58.9		15.3	2.4	
M_4	3.8646	2.4	45.1		1.6	75.6		0.8	19.7		1.7	99.5	

Major = Semi-major axis of tidal ellipse in cm^{-1}. Semi-minor axis not listed.
Direction = True north. Phase = Greenwich epoch. Amplitude in cm.
Station locations specified in Cheng & Gartner, 1984.

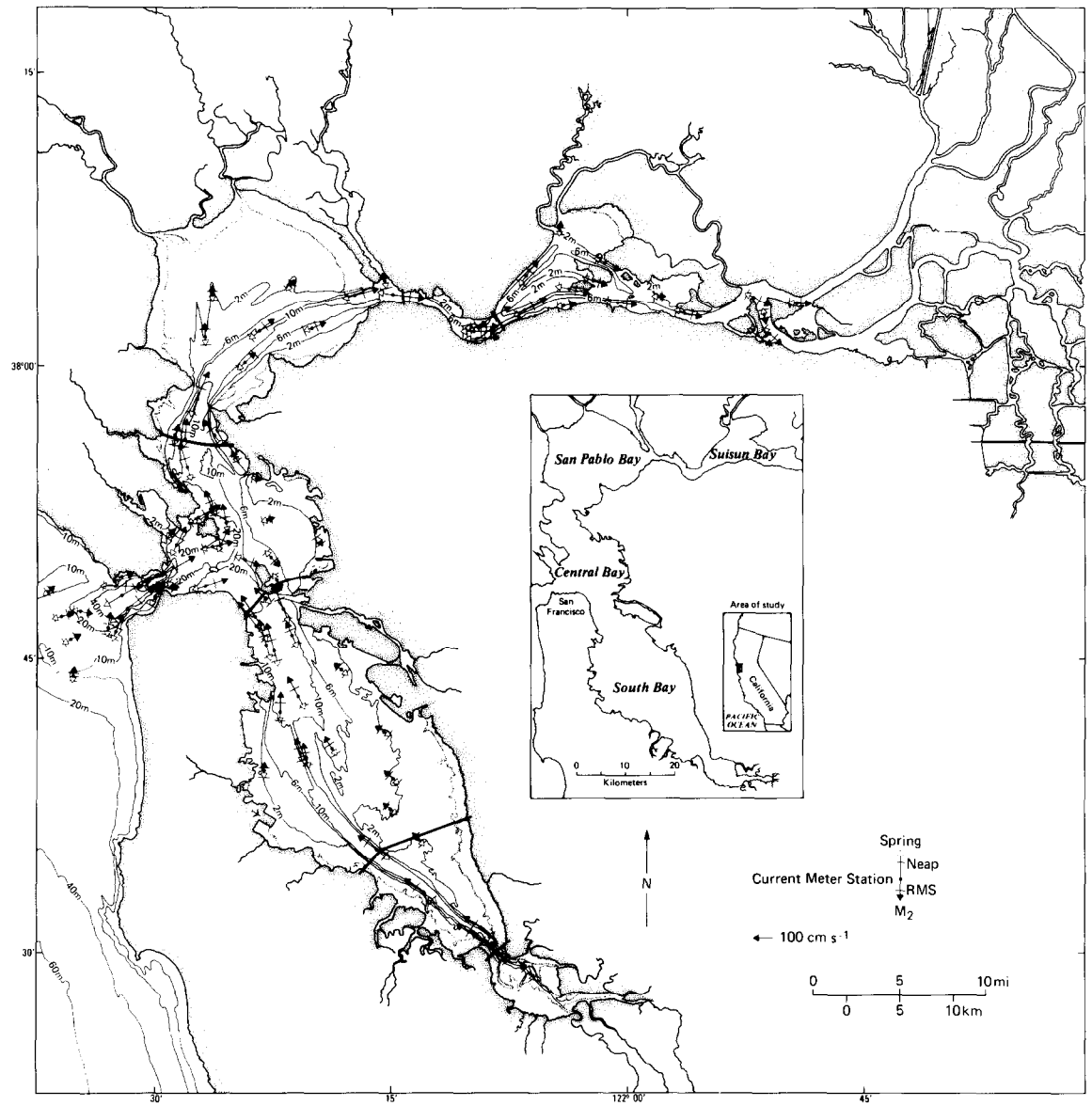

Fig. 6. Spatial distribution of tidal currents as represented by M_2, RMS current speed, and the estimated spring and neap current vectors in the principal direction.

(representing the water movements over the shoal) the tidal excursion is about 7.8 km. The tidal excursion also varies with the spring and neap tides. The estimated spring and neap tidal current vectors (Fig. 6) can be used to give estimates of the spring and neap variations of tidal excursion. For instance, in the channel of South Bay, the neap amplitude is about half of the spring amplitude. For a spring excursion of 13 km, the neap excursion is about 7 km. The drogue studies of Kirkland & Fischer (1976) in a hydraulic physical model of the bay also illustrate these concepts.

Low-frequency variation in sea level and currents

Introduction

Physical processes that cause low-frequency variations in sea level and in currents can be divided

into (1) nonlocal forcing whose primary component is the coastal variation in sea level that arises from meteorological influences, and (2) local forcing whose primary components are wind stress on the water surface, freshwater inflow, and tidal currents interacting with the complex bay geometry. As our primary interest is in currents and mixing, low-frequency changes in sea level at Golden Gate by nonlocal forcing are of secondary importance. The effects of these changes upon currents are usually small because of their low amplitude and long time scales (>several days).

Local forcing then includes the dominant mechanisms for driving the residual flows, although there is considerable variation in both space and time of the relative importance of specific processes. In the northern reach the longitudinal density gradient drives an estuarine circulation in the channels, and the spatial variation in tidal amplitude creates a tidally-driven residual circulation. The effects of wind can be important, especially in the shoals. In contrast to the northern reach, South Bay exhibits a balance between wind-driven circulation and tidally-driven residual circulation for most of the year. During winter, however, there can be sufficient density variations to drive multilayered flows in the channel. These forcing mechanisms are described in more detail below.

Conceptual model for sea level and currents

The bay is a partially to well-mixed estuary extending from Golden Gate to the confluence of the Sacramento and San Joaquin Rivers, with South Bay existing as a tributary estuary (Fig. 1). Consequently, South Bay responds to tidal exchanges and density differences with Central Bay, which are in turn governed largely by the water circulation in the northern reach.

The northern reach. The region of the bay between Suisun Bay and Golden Gate is in its least transient condition in late summer when river flows are controlled by water diversions in the various state and federal water projects (Conomos, 1979; Orlob, 1977). The northern reach is nearly well-mixed in the vertical with an estuarine circulation driven by the horizontal density gradient (Peterson *et al.*, 1975). Conceptually, the residual flow can be separated into the horizontal mean flow (vertically uniform) driven by processes that include freshwater inflow and tidal forcing (Fischer & Dudley, 1975), and a flow that is density driven. The tidally-driven residual flow reaches its maximum amplitude during spring tides, as this is when the forcing has its greatest effect. The density-driven flows, on the other hand, are weakest during spring tides due

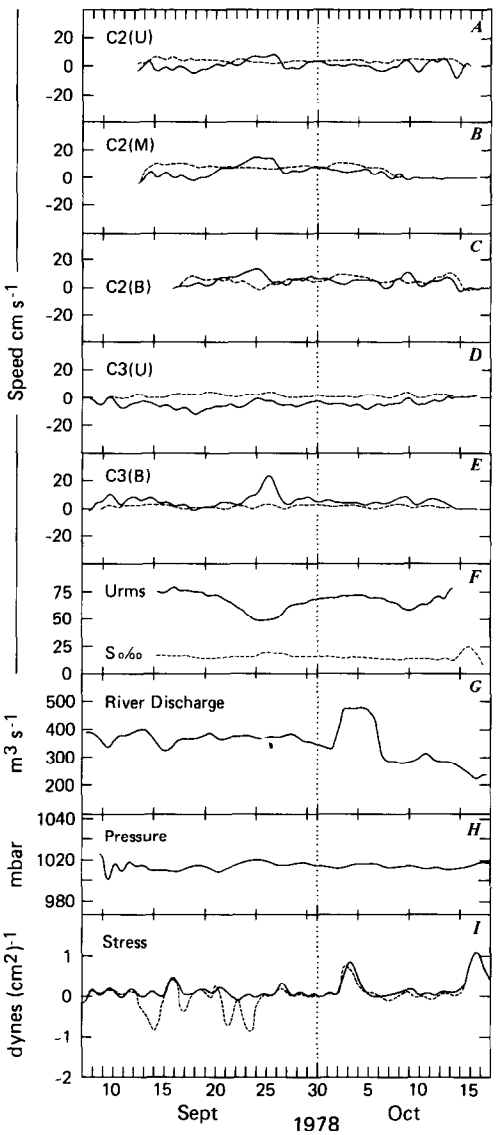

Fig. 7. Low-pass filtered currents at stations C2 and C3 (Fig. 8) after rotating into the local bathymetry: – longitudinal speed, positive upstream; -- transverse speed, positive 90° to the left of upstream. The low-pass filtered root-mean square tidal speed and salinity at C_2. Daily averages for Sacramento and San Joaquin River inflows. Atmospheric pressure at Travis Air Force Base, and wind stress calculated from Travis wind speed and direction: positive north (—), positive east (– – –).

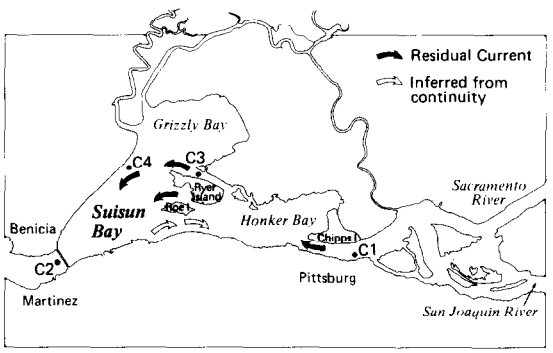

Fig. 8. Tidally-driven residual circulation (depth mean) in the horizontal plane in Suisun Bay as determined from current meter data collected at stations C1 to C4 and inferred from continuity considerations.

to enhanced vertical mixing. During late summer, freshwater inflow is relatively low and contributes approximately 1 cm s^{-1} to the net flow (cross-sectionally averaged). This component of the flow can be neglected with respect to the larger tidally-driven and density-driven flows (Fig. 7A–C).

A counter-clockwise rotating tidally-driven residual flow in Suisun Bay (Fig. 8; Walters & Gartner, 1985) is inferred from current-meter data (Fig. 7). During spring tides, a down-estuary flow across the northern portion of Suisun Bay results from the tidally-driven residual flow dominating the density-driven up-estuary flow (September 17, Fig. 7D, E). During neap tides, the density-driven flow dominates because of decreased vertical mixing (higher density-current speeds) and weakened residual flow (September 25, Fig. 7D, E). A comparison of meteorological and current meter data has failed to reveal any wind-driven component in the residual circulation in Suisun Bay.

The horizontal circulation pattern in San Pablo Bay is unknown. The geometry suggests a clockwise circulation driven by a tidal jet at the eastern and western boundaries. Because of the shallow depth, the circulation probably has an important wind-driven component, as suggested by observations of substantial wind setup in San Pablo Bay (Walters & Gartner, 1985).

It is presently difficult to establish the magnitude of the density-driven estuarine circulation. Because of the presence of heavy ship traffic, it is difficult to deploy current-meter moorings with sufficient resolution in the vertical, particularly near the surface. The available data are primarily from the landward flowing bottom layer, so it is not possible to discriminate between the horizontal flow which is unidirectional with depth and the density current which reverses direction with depth. Data collected during summer, with river inflows of 300–400 m^3 s^{-1}, suggest a typical density current speed of about 15 cm s^{-1} in Carquinez and San Pablo Straits and about 10 cm s^{-1} in upper and eastern Suisun Bay (Peterson *et al.*, 1975).

Winter flow conditions are characterized by large peaks in river inflow followed by a slow reduction in discharge (Fig. 3; Conomos *et al.*, 1985). During large peak inflows (flows $>10^3$ m^3 s^{-1}), Suisun Bay becomes a riverine rather than an estuarine basin, and the flows are essentially unidirectional seaward. For large inflows ($>10^4$ m^3 s^{-1}) a salt wedge develops near Carquinez Strait (Conomos *et al.*, 1985). The estuary downstream is stratified with a marked depression in surface salinity in Central Bay. The low salinity surface waters form a turbid surface layer that flows seaward through Raccoon Strait and around Angel Island (Fig. 1). With the reduction in river inflow during spring, the estuary becomes partially stratified, then well mixed vertically, and the salinity increases on a monthly time scale. At Golden Gate, the water is usually well mixed vertically over much of the water column because of the large tidal currents and resultant mixing.

The complex geometry and bathymetry at Golden Gate causes relatively complex residual currents. The inflow follows the depths along the south shore of the entrance to the bay, whereas the surface outflow tends to follow the more shoal areas and is concentrated toward the northern shore. Superimposed upon this circulation pattern is a tidally-driven residual flow that is directed up estuary in the center of Golden Gate, and toward the ocean along the shores.

The southern reach. South Bay, during its least transient state in late summer, can be described as a tidally oscillating lagoon. Inferences from the current-meter data indicate a southward-flowing current along the northeastern side of the entrance to South Bay and an outflow over the remainder of the entrance (Walters, 1982). This flow is consistent with inertial effects deflecting the flooding tidal flow southward along the eastern shore at the entrance to South Bay and an ebb flow uniformly

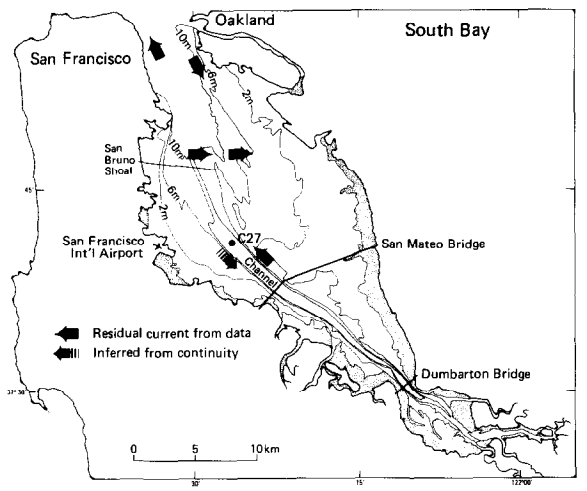

Fig. 9. Tidally-driven residual circulation (depth mean) in the horizontal plane in South Bay as determined from current meter data collected between 1979 and 1982 and inferred by continuity considerations.

spread over the entrance (Fig. 9).

Available measurements lead us to infer a tidally-driven residual current northward along the east side of the main channel and eastward along the northern slope of San Bruno shoals (Fig. 9; Walters, 1982). Horizontal residual flows south of San Mateo Bridge appear to be extremely weak and are not measurable. At both the north and south ends of South Bay, a tidally-driven secondary flow manifests itself as a rolling motion whose axis lies along

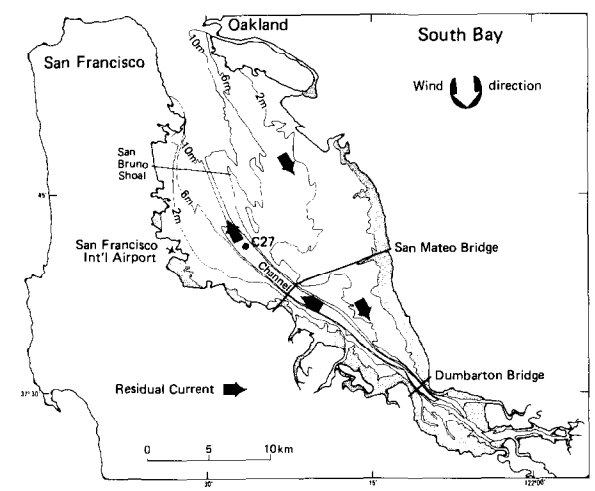

Fig. 10. Wind-driven circulation in South Bay with a northerly wind. These are depth averaged flows with a surface flow over the entire bay and a return flow up the channel.

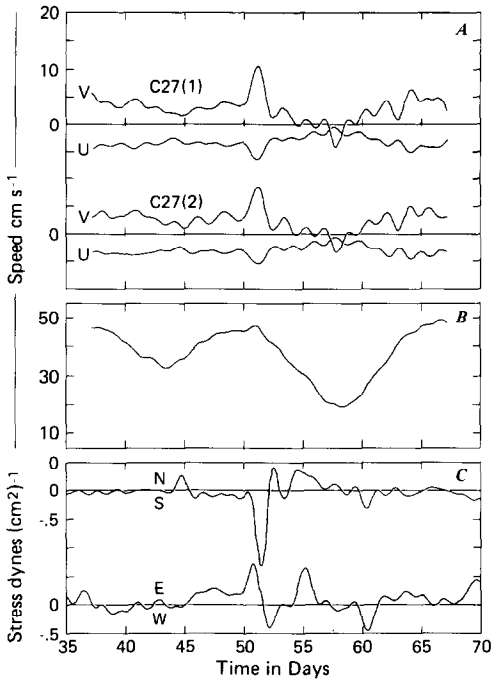

Fig. 11. Velocity (A), root-mean-square (RMS) tidal current speed (B), and wind stress (C). The current velocity is calculated from the low-pass filtered u and v velocity components for the two current meters at C27: (1) top meter; (2) bottom meter. The RMS tidal current is calculated from the data at C27, the top meter. The wind stress components are calculated using wind data from San Francisco Airport; N-S, north-south component; E-W, east-west component (after Walters, 1982).

the longitudinal axis of South Bay. In the north, the rolling is in a counterclockwise sense, looking north, and in the south at Dumbarton Bridge, the rolling is in the opposite direction.

We are uncertain about the flow patterns in the shoals west of Oakland and on the western side of the channel. The flow appears to be moving southward in the latter case, with the result that the flow in the channel describes a counterclockwise rotation along the depth contours. If this is true, this flow would account for the observed longitudinal dispersion along the channel (see mixing section).

The wind-driven flows are characterized by a wind-driven surface layer and a return flow in the channels (Fig. 10). Current pulses that are highly correlated with wind stress and oriented in nearly the opposite direction can be detected (Fig. 11; Walters, 1982). Because of the configuration of South Bay, there are some wind directions (northerly or southerly) that lead to much larger perturba-

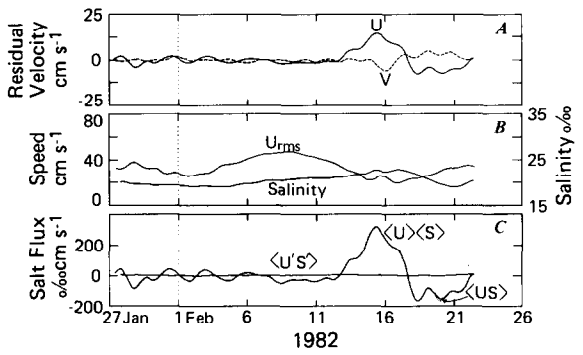

Fig. 12. A time series of (A) residual velocity, (B) salinity and root-mean-square (RMS) current speed, and (C) salt flux components at a current meter station south of San Bruno Shoal (Fig. 1). u, low-pass filtered velocity along channel, positive up-estuary (south); v, lateral velocity positive to the left of u (east). U_{rms}, RMS current speed; S, low-pass filtered salinity; <us>, low-pass filtered salt flux (see Equation 8); <u><s>, mean advection of the mean salt field; <u's'>, tidal correlation component of the salt flux (small in this case).

tions in the ambient currents.

The flow regime of South Bay becomes much more dynamic with the onset of winter storms. With the first pulse of low salinity water through the northern reach, the density of Central Bay waters is depressed. Hence, the saltier, higher density water in South Bay effectively flows seaward (northwestward) along the bottom and is replaced by lower density water flowing landward (southeastward) near the surface. The strength of these currents depends upon the magnitude of the freshwater inflow, the intensity of vertical mixing and hence the tidal amplitude. During the periods of neap tides, vertical mixing is reduced and the density currents are relatively strong (up to 15 cm s^{-1}), whereas during spring tides these currents are weak (only a few cm s^{-1}).

With the decline of river inflow during late spring, the salinity in Central Bay increases toward oceanic values. If the water density there becomes greater than that in South Bay, the circulation reverses with intruding water near the bottom (Fig. 12) and outflowing water near the surface. An interesting variation of this flow pattern leads to a three-layered flow similar to that described for Baltimore Harbor (Cameron & Pritchard, 1963). When the water in Central Bay is stratified, mixing over the San Bruno shoals can create a water type with a density intermediate between that of the

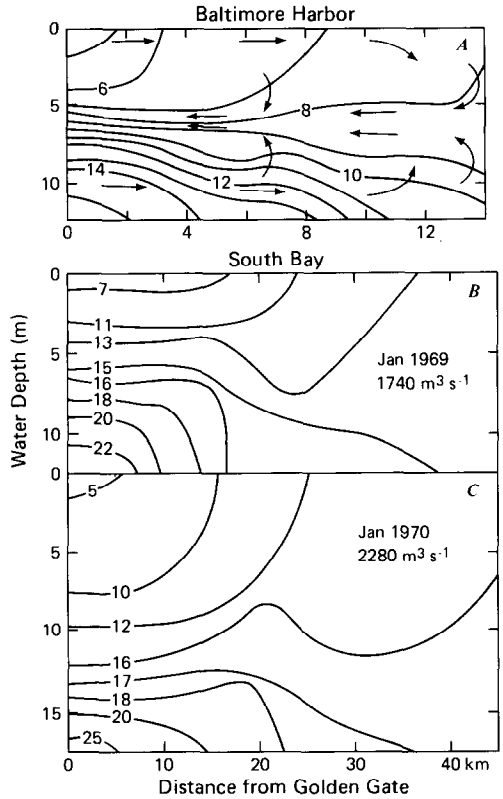

Fig. 13. Longitudinal salinity section of Baltimore Harbor (A), after Cameron & Pritchard (1963), compared with those of South Bay (B, C). All panels modified after Conomos (1979).

surface and bottom waters. Water then flows seaward as a mid-depth layer with inflowing (landward) bottom water driven in by the density gradient and inflowing (landward) surface water driven in by the surface pressure gradient (Fig. 13, 14).

There are usually several freshwater peaks during a normal winter (see Fig. 3; Conomos *et al.*, 1985) so that the flow pattern is highly transient, shifting between the different patterns. After the last river inflow peak of winter, salinity in South Bay increases steadily to oceanic values. During this period the flow can alternate between two- and three-layer flow with high salinity bottom water flowing steadily landward. There is usually a well-developed estuarine circulation pattern over most of the channel.

The scenario presented here becomes somewhat more complicated in very wet winters when there are large inflows northward from Coyote Creek and Guadalupe River at the extreme south end of the bay (Fig. 1). Then the tapered southern end of

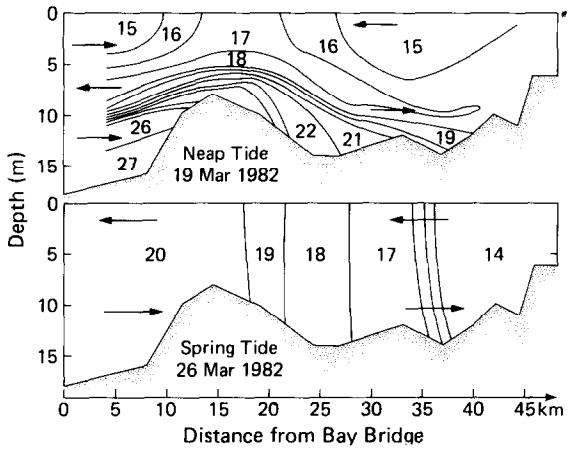

Fig. 14. Vertical distribution of salinity in South Bay during spring and neap tidal cycle periods, March 1982. Data uncorrected for tidal variations.

South Bay responds locally as a partially mixed estuary with a typical estuarine circulation pattern. Although this pattern can be inferred by the characteristic salinity distribution (Fig. 14), little is known about this flow regime.

Eventually, the winter flow regime in South Bay, driven by density currents, gives way to summer isohaline conditions and the resultant weak summer tidally-driven and wind-driven residual flows.

Physical processes

To examine the various physical processes contributing to low-frequency motions through a simple mathematical framework, we divide the discussion into processes that generate (1) circulations that vary horizontally but are more or less uniform with depth (such as freshwater flowing down a channel), and (2) circulations that vary with depth (such as estuarine circulation). Thus, we may describe the approximate motions in terms of a two-dimensional (horizontal) set of equations and a one-dimensional (vertical) set of equations. In the first category we lump tidally-driven residual flows, freshwater flows, and depth-mean, wind-driven flows. The second category includes density-driven flows and the vertical variation in wind-driven flows.

The appropriate time-averaged equations for the depth-integrated residual flow can be written as:

$$\frac{\partial \eta}{\partial t} + \nabla \cdot [(H + \eta)\, u] = -\nabla \cdot \langle \eta' \underline{u}' \rangle \qquad (1)$$

$$\frac{\partial \underline{u}}{\partial t} + \underline{f} \times \underline{u} + g\nabla\eta \frac{kU_{rms}}{(H+\eta)} \underline{u} = \underline{\tau}_t + \underline{\tau}_w - \frac{1}{2} \frac{g(H+\eta)}{\rho} \nabla\rho \qquad (2)$$

with the appropriate boundary conditions: sea level specified at open (sea) boundaries, zero normal velocity at solid boundaries, and inflow at river boundaries. Here $\underline{u}$ is the time-averaged horizontal velocity, η is the time-averaged sea level measured from its mean H, $\langle\rangle$ denote a time average or a suitable low-pass filter (Walters & Heston, 1982), the primes denote the tidal period variations from the mean, $\underline{f}$ is the Coriolis parameter, g is gravitational acceleration, k is a bottom-friction coefficient, U_{rms} is the root-mean-square current speed, τ_t is the tidal stress, τ_w is the wind stress on the surface, and ρ is water density. The dominant component of U_{rms} is the tidal-current speed, although the river-current speed can dominate in the upper northern reach in winter. The tidal stress (τ_t), the time average of the nonlinear advective terms, can contain some second-order terms from the nonlinearities in the bottom friction term (cf. Uncles, 1982 or Walters & Cheng, 1980). We thus have a set of governing equations that have four distinct forcing terms: the tidal nonlinearities, wind stress, boundary forces (inflow or sea level changes), and density differences. Each of these resultant circulations can be superimposed to give a realistic flow that is observed in field data. This comparison is, unfortunately, not trivial.

Tidally-driven residual flow. Divergence of the wave transport and tidal stress both contribute to the tidally-driven residual circulation. The divergence of the wave transport (the last term in Equation 1) can be conceptualized as follows. As a tidal wave propagates up an estuary, there is a net landward flow of water. This flow causes a sea-level setup in the upper estuary that in turn drives a compensating flow. For steady conditions in a one-dimensional estuary with an absence of river inputs, the wave transport speed and the return flow speed are equal in magnitude and opposite in sign. As the tidal amplitude of the wave varies over a spring-neap tidal cycle, the wave transport also varies and

hence, causes a variation in sea-level setup. From an analysis of sea-level data, the variation in setup is about 10 cm in Suisun Bay (Walters & Gartner, 1985). Using sea-level and current-meter data, we estimate the wave-transport speed at about 1–2 cm s^{-1}, much less than the speed associated with currents driven by tidal stress or density gradients.

Tidal stress, which also contributes to the tidally-driven residual current, includes contributions from the time-averaged advective term and time-averaged bottom stress term (Walters & Cheng, 1980; Uncles, 1982). This term apparently drives the net counter-clockwise circulation in Suisun Bay (Fig. 8), the clockwise circulation in San Pablo Bay, and various eddies around Golden Gate. The magnitude of the residual circulation in Suisun Bay is about 10 cm s^{-1}; the magnitude in San Pablo Bay is unknown. Although we cannot detail the net circulation in Central Bay, we have detected residual flows near Golden Gate with speeds of up to 35 cm s^{-1} (unpublished data).

The wave transport component in South Bay is small because of the standing-wave nature of the tidal wave (the time-average of the product of η' and u' is small as they are nearly in quadrature). Numerical models (Walters & Cheng, 1980) have verified that the existing currents are driven primarily by the tidal stress term. The actual flow speeds are both small (about 5 cm s^{-1}) and relatively complicated due to the small spatial scales of the channel width and the presence of San Bruno Shoal. The residual currents appear to follow the bathymetric contours.

Wind-driven circulation. The effects of winds are represented in Equation 2 through the surface-wind stress (τ_w) which is proportional to the square of the wind speed. The magnitude and character of the resultant circulation patterns vary dramatically from embayment to embayment depending upon the direction of maximum fetch and the presence of shoals. In Suisun Bay the winds are predominantly easterly or westerly reflecting reversals of land and sea breeze (Conomos, 1979; Fig. 6). No correlation between wind and currents has been noted for summer wind conditions (Walters & Gartner, 1985).

The conditions in San Pablo Bay are somewhat different. Because of the trend of the coastal mountains, strong northwesterly and southerly winds can create a substantial (10–20 cm) setup in sea level between the northern and southern shores of San Pablo Bay (Walters & Garner, 1985). This setup is normal to the trend in the bottom topography and generates currents of unknown magnitude.

The effects of wind forcing are better understood in South Bay. The wind direction and speed there are controlled to a large degree by the coastal mountains containing several gaps that tend to funnel the westerly winds (Conomos, 1979; Conomos *et al.*, 1985). In summer, the westerly air movements are dominated by a sea breeze with a marked diurnal variation. In winter, however, wind speed is reduced and modified by storms with typically southerly to westerly winds. The winds generally cause a surface flow of water in the direction of the wind and a return flow largely confined to the channels (Walters, 1982). For westerly to northwesterly winds the return flow in the channel is to the northwest, whereas for southeasterly winds this flow is to the southeast. If generated by sufficiently strong winds, these flows can dominate the tidally-driven residual circulation.

Because of the configuration of South Bay, some wind directions are more effective in driving a return flow in the channel. When northerly to northwesterly winds prevail there is a wind-generated setup along the deep channel that causes a strong return flow. Southeasterly winds reverse the setup and create a strong flow down the channel. For westerly winds, however, the sea level setup is normal to the channel and creates a condition whereby the return flows are weak in the shallow water to the east. This type of response probably also occurs in San Pablo Bay, with water-flow directions shifted in response to the trend of the channel.

River-inflow effects. The forcing from river inflows into the bay system appears in the flow boundary conditions for Equation 2. During winter the circulation in Suisun Bay is dominated by large peak flows. Current speed varies proportionately with water depth, with large speeds in the main channels. For the most part these flows follow bathymetric contours. Typical speed varies from >50 cm s^{-1} during flow peaks to 1 cm s^{-1} during low flow summer conditions. In South Bay the effects of freshwater inflows are negligible except in the very southern part during extreme environmental conditions (Conomos, 1979; Fig. 10).

Density-driven estuarine circulation. The three-dimensional estuarine circulation is driven by the

horizontal density gradients and is confined to the channels and Central Bay. It is relatively well developed in deep water (>10 m) and is weak or absent in shallow water over the lateral shoals and channel shoals (San Bruno and Pinole Shoals). The strength of the density current varies proportionately with the horizontal density gradient and inversely with the magnitude of vertical mixing. Note that density currents exist even when the estuary is well-mixed vertically. The problem can be formulated simply as

$$\frac{1}{\rho}\frac{\partial p}{\partial x} = -g\frac{\partial \eta}{\partial x} + gz\frac{\partial \rho}{\partial x} = N\frac{\partial^2 u}{\partial z^2} \qquad (3)$$

where ρ is density, p is pressure, and N is eddy viscosity. An analytical solution for a uniform channel is given by Officer (1976)

$$u = \frac{1}{N}\left[\frac{g}{2}(H^2 - z^2)\frac{\partial \eta}{\partial x} - \frac{g}{6\rho}(H^3 - z^3)\frac{\partial \rho}{\partial x}\right] \qquad (4)$$

Hence, there are smaller density currents because of the relatively large vertical mixing (and large N) during spring tides and larger density currents because of the smaller vertical mixing during neap tides. Because of the seasonal variations of water density in response to variations in freshwater inflow, the density currents exhibit a strong seasonal variation. The density current speed in Suisun Bay during late summer (river discharge of 350 $m^3 s^{-1}$) is about 10 cm s^{-1}. During winter peak flows the speeds are probably about 15–20 cm s^{-1} in Carquinez Strait. The current speed in the channel of San Pablo Bay is slightly higher than these estimates (about 15 cm s^{-1} in summer). In South Bay the density currents are absent in summer due to the lack of significant river inflows, and are about 15 cm s^{-1} in the channel south of San Bruno Shoal during winter.

Interactions. The amount of vertical mixing and the magnitude of the bottom stress are controlled by the amplitude of tidal currents because most of the energy for mixing is derived from the tides. In addition, because tidal stress varies as a power of the tidal-current amplitude (Walters & Cheng, 1980; Uncles, 1982), the spring-neap variation in the tides causes a corresponding variation in the residual flows. It can be seen in Equation 2 that the mechanism which connects these time scales is the nonlinearity in the physics of the system: the variation in current speed modulates the magnitude of the bottom friction and the tidal stress (τ_t). With some simplification of Equation 2, it becomes apparent that the residual current is directly proportional to the tidal-current amplitude. This concept, pursued by Tee (1977), is also valid for San Francisco Bay.

There is also a semi-annual variation in tidal amplitudes with the weakest tides occurring during April and October (Conomos *et al.*, 1985). Walters & Gartner (1985) examined current-meter data collected during this neap tide in October 1978 and found a sharp decrease in the tidally-driven residual flows, an increase in the speed of the estuarine circulation, and an increase in stratification. A case of topographic blocking in the stratified flow was also detected during this period.

The interactions between tidal-current amplitude and the speed of the estuarine circulation can be better seen by considering an estuary whose hydrodynamics are governed by a balance between the horizontal pressure gradient (including both sea-level slope and density gradients) and vertical variation in stress. Simple analytical solutions to these relationships (Officer, 1976) show that the strength of the estuarine circulation varies inversely with the eddy viscosity coefficient (Equation 4). In addition, Uncles (1982) has found that the eddy viscosity is proportional to the mean-tidal current amplitude. Hence, the estuarine circulation also varies as the inverse of the mean (1- or 2-d average) tidal amplitude. The modulation of the estuarine flow by the amplitude of the tidal currents has been examined by Budgell (1982) for a dramatic case in Chesterfield Inlet, Canada, by Walters & Gartner (1985) for the northern reach of San Francisco Bay, and herein (Fig. 12) for South Bay.

Similarly, wind-generated waves can modify the circulation in the shoal areas through the same nonlinear mechanisms described above. Wind-wave effects are comparable to tidal effects in selected areas and affect the mean flows through these mechanisms. However, different time scales – a diurnal variation associated with the sea breeze, and a 3- to 4-d variation associated with storms – are induced into the flow.

Mixing

Introduction

Mixing as discussed herein includes both diffusive and dispersive processes. In the consideration of solute and particulate distributions, one must be concerned with where the water goes (circulation), how it mixes, and what sources and sinks exist. Sources and sinks are considered elsewhere (Conomos *et al.*, 1979; Peterson, 1979; Peterson *et al.*, 1985). This paper establishes the foundation for the first two concerns. Further, we will only concern ourselves with salinity as being representative of a conservative solute.

For simplicity, we treat the discussion of the salinity distribution in the bay as a mixing between two water 'types' - river (freshwater) inflow (0‰) from the Sacramento-San Joaquin River and various creeks and outfalls, and water of oceanic salinity (34‰) at Golden Gate. The amount of mixing and the spatial distribution of the mixing processes depend upon the details of circulation and vertical exchange rates. Since energy input for mixing is derived from the tides, wind, and freshwater inflows, the important time scales depend upon both the time scales associated with solute variations at the boundaries and those associated with the physical forcing mechanisms. The spatial scales of variations are dependent upon the configuration of the bay and are strongly influenced by the bathymetry that is characterized by relict river channels. Larger spatial scales are associated with the extensive shoal areas in San Pablo and South Bays.

An understanding of mixing is crucial to understanding solute transport and distributions in the bay. As will be seen in the following discussion, our knowledge of mixing is, unfortunately, in its infancy.

Conceptual model of mixing

We separate mixing into horizontal and vertical components that parallel the separation of the circulation into a horizontal mean flow and vertical variations in the flow. We examine horizontal mixing over length scales of 100 m or larger and vertical mixing over length scales of a few meters or larger. We do not consider mixing across fronts. Whereas some discussion of tidal-period mixing is necessary, our focus is upon time periods of several days and longer. At Golden Gate, the instantaneous salt flux is dominated by advection by the tidal flow. Low-pass filtering the salt-flux data shows that the low frequency or residual component of the salt flux at a particular point in the cross section is dominated by the advection of the mean-salt field by the mean flow. The portion of the salt flux arising from correlations between tidal period fluctuations is generally small (see Processes section). Because there are insufficient data to examine the salt-flux components over the entire cross-section such as was done by Hughes & Rattray (1982) for the Columbia River, we cannot determine whether lateral variations in velocity or vertical variations in velocity are most important to the net salt flux. Intuitively, both can be important in different seasons.

Mixing in the northern reach is dependent upon the presence of large shallow bays connected by narrow and deep straits. The straits have a strong gravitational circulation as well as secondary currents which describe a rolling motion about the axis of the strait. The large bays, however, generally have a tidally-driven residual circulation in the horizontal direction. Where the estuarine circulation is strong, the salt flux is carried by the mean advection of the salt field and the vertical variations in the mean flow are the major terms in the net salt flux. Where large salinity gradients are present (i.e., as in upper Suisun Bay in summer), the tidal correlation portion of the salt flux is of the same order as the advective part.

A special case occurs in San Pablo Bay where Pinole Shoal (Fig. 1) blocks the estuarine circulation in the main channel. There appears to be a dispersive mechanism that 'pumps' high salinity water over the shoals on flood tides, and returns more brackish water during ebb tides. In addition, the flood tide sweeps across the large shoal area north of the channel and forces solutes and particulates into the channel at the west end of Carquinez Strait. On ebb tide, the shoal area drains into San Pablo Strait. This pumping mechanism thus causes a lateral exchange between the channel and shoals.

The salt flux in Suisun Bay is generally a balance between the mean-advective portion and the tidal-correlation portion of the flux. During extreme neap tides such as usually occur in October, parts of Suisun Bay will stratify and the flux is dominated by the mean-advective component from the estua-

rine circulation (Walters & Gartner, 1985).

There are insufficient data to evaluate the relative importance of lateral variations in salt flux versus vertical variations in salt flux as they contribute to the net salt flux. Furthermore, there are no data for winter peak river flow periods, so the results above may hold only for the summer conditions of controlled low river inflows.

The evaluation of mixing in South Bay during summer is difficult due to the absence of a suitable tracer solute. As South Bay is nearly isohaline, the salt flux is dominated entirely by the mean-advective component. Calculations using the measured lateral variations of velocity in the channel provide longitudinal exchange coefficients which are of the same order as those used by Fischer (1978) in a box-model analysis. Fischer also reported low values for exchange coefficients across San Bruno Shoal that would be predicted by the absence of significant residual flows there. The exchange between the channel and the lateral shoals is not well understood although the tidal currents seem to sweep the shoal to the east of San Bruno Shoal and transport solutes and particulates into the channel north of San Mateo bridge. South of the bridge the tides pump water laterally directly onto the shoals. The exchange rates are unknown.

During and after peak river discharge, the mixing in South Bay becomes much more dynamic (McCulloch *et al.*, 1970; Imberger *et al.*, 1977; Conomos, 1979). Whereas in summer there is a weak residual inflow along the east side of the mouth of South Bay and an outflow on the west, there can be a strong density-driven current in winter. The latter current greatly enhances mixing between Central and South Bays and complicates the mixing dynamics. Following a discharge peak, the salinity of Central Bay waters will reach a minimum with a time lag of 6 days or less (Conomos, 1979; Fig. 12). As the salinity in Central Bay is reduced, there is higher salinity (and higher density) water in South Bay. The longitudinal pressure gradient causes a density current to flow out of South Bay such that there is a net exchange of both water mass and salt. These flows, and hence the exchanges, are stronger during neap tides when vertical exchanges of momentum and salt are reduced (Walters, unpublished data). South Bay is often stratified during these periods of neap tides (Fig. 14). With a time scale of a few days to a week, the salinity in South Bay will equilibrate to that in Central Bay; this equilibration tends to minimize the density current exchanges.

With the reduction in river inflow in late spring and summer, the salinity of Central Bay waters increases and thus drives a density current into South Bay. The saline water seems to intrude primarily into the channel, whereas the less saline, near-surface water seems to flow out of the remainder of the lateral cross-section. Again, the density currents are enhanced during neap tides and reduced during spring tides in response to tidal mixing in the vertical direction (Fig. 12). During this recovery period, South Bay remains tightly coupled to Central Bay; that is, the time scales for exchanges with South Bay are shorter than the time scales associated with the recovery of the hydrograph (weekly versus monthly) and hence the salinity distribution in Central Bay.

During periods when there is sufficient vertical mixing in South Bay over San Bruno Shoal to remove stratification, South Bay waters have a density intermediate between the low-salinity surface water and high-salinity deep water in Central Bay (Fig. 13). In response, a three-layer flow develops. This flow pattern appears to be less effective than the flows during neap tides in promoting exchanges with Central Bay. As the river inflow decreases to summer conditions, South Bay eventually equilibrates with the oceanic waters of Central Bay. For these conditions, the exchange rates are reduced and depend upon the weaker tidally-driven residual flows.

Processes for horizontal mixing

We examine solute distributions and mixing processes within the framework of the time-averaged equation for solute transport

$$\frac{\partial c}{\partial t} + \underline{u} \cdot \nabla c - K\nabla^2 c + \langle \underline{u}' \cdot \nabla c' \rangle \pm S = 0 \quad (5)$$

where C is the time-averaged solute concentration, u is the time-averaged velocity, K is the eddy diffusion coefficient, S is the source-sink term, and $\langle u' \cdot \nabla C' \rangle$ is the tidal dispersion term, for which the prime denotes tidal period variations and brackets denote a suitable time average. We neglect nonlinear correlations between the diffusion coefficient and concentration over tidal-time periods.

Processes that contribute to mixing, then, are the advection of solute, its diffusion away from high concentrations, and the tidal dispersion of the solute. It is reasonable to assume that advection and dispersion control horizontal mixing whereas vertical diffusion controls vertical mixing.

Our analysis of the salt flux is limited by two factors: (1) current meters cannot be deployed in the uppermost three meters of the water column because of heavy shipping traffic, and (2) usually only one current-meter array has been deployed at a given cross-section. Hence, we cannot quantify the importance of lateral variations in salt flux nor the contribution of the surface-flowing layer to the overall flux. We can, however, examine the relation between the advective and dispersive components of salt flux at a particular point and extrapolate vertical variations where the data permit.

For the purposes of this analysis we decompose the velocity and salinity into both low-frequency and tidal components:

$$u = \langle u \rangle + u' \tag{6}$$

$$s = \langle s \rangle + s' \tag{7}$$

where u is the longitudinal velocity component, s is salinity, $\langle\rangle$ denote a suitable low-pass filter (Walters & Heston, 1982), and the prime denotes the tidal period variations. The low-frequency variations in salt flux (F) at a discrete point are

$$\langle F \rangle = \langle us \rangle = \langle u \rangle \langle s \rangle + \langle u's' \rangle \tag{8}$$

where $\langle u \rangle \langle s \rangle$ is the advection of the mean salt field by the mean velocity, and $\langle u's' \rangle$ is the dispersive flux which depends upon the correlation between the tidal variation in velocity and salt concentration. In general, $\langle u \rangle \langle s \rangle$ dominates the salt flux whereas the second term, $\langle u's' \rangle$, can be of comparable magnitude in the northern reach but is usually smaller although not negligible (Walters & Gartner, 1985). Most data records show a spring-neap variability in the flux due to variability of the mean flow in $\langle u \rangle \langle s \rangle$ and variability in the tidal velocity in $\langle u's' \rangle$. The data for South Bay show that the mean advection term, $\langle u \rangle \langle s \rangle$, dominates the flux (Fig. 12C). Although not observed, we suspect that the second term can be important at the northern boundary of South Bay during periods of high inflows from the Sacramento and San Joaquin Rivers.

A somewhat complicated mixing mechanism is apparent where shoal areas occur in the main channel (i.e. San Bruno and Pinole Shoals). For example, to the east and west of Pinole Shoal the estuarine circulation is well developed in Carquinez and San Pablo Straits. On the shoal, however, this circulation is weak or absent because of the shallow water depth. The salt flux appears to be dominated by a dispersive mechanism that effectively 'pumps' saline water over the shoal on the flood-tide cycle and returns more brackish water on the ebb. The details of this simple picture are complicated by the presence of the shoals to the north.

The San Pablo Bay water movements over a tidal cycle are as follows. As the flood-tide cycle begins, the waters incoming from San Pablo Strait flow onto the shoals with some shoal water spilling into Carquinez Strait in the east. As the flood tide progresses, the water becomes more saline and flows into Carquinez Strait because of the small water volume over the shoals of San Pablo Bay. When the tide begins to ebb, the lower-salinity water on the shoals ebbs first followed by higher salinity water in Carquinez Strait, and finally followed by the brackish water. This double peak in salinity values

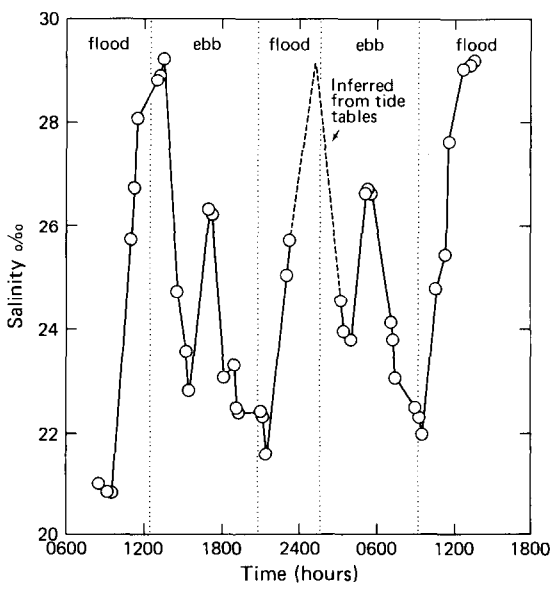

Fig. 15. Surface-salinity distribution at a representative station in eastern San Pablo Bay, 23–24 September 1980. Data from California Department of Fish and Game.

(Fig. 15) during each tidal cycle suggests the presence of a dispersive mechanism. This suggestion is reinforced by the observations on Pinole Shoal of discrete, high salinity water masses with length scales of the order of 100 m. These results must be considered preliminary as we lack sufficient data to closely examine this mixing mechanism.

In South Bay, a similar pumping mechanism appears to occur over San Bruno Shoal during winter where there can be a well-developed estuarine circulation south of the shoals and poorly developed over the shoals. This circulation is currently under study.

Which, then, are the dominant processes controlling the net salt flux through a given cross-section of the bay? A convenient place to begin is with a discussion of the flux at Golden Gate. Using the data from a current meter array that was deployed at Golden Gate, we can examine the salt flux through a section of unit width. Letting h denote the water depth and the overbar a depth average, the salt flux F_h can be expressed as

$$\langle F_h \rangle = \langle \overline{ush} \rangle \tag{9}$$

where u is the velocity and s is the salinity. We can further decompose the dependent variables as

$$\langle u \rangle = \langle \bar{u} \rangle + \langle u \rangle_z \tag{10}$$

$$\langle s \rangle = \langle \bar{s} \rangle + \langle s \rangle_z \tag{11}$$

where the overbar denotes a depth average, and the filtered variable has been written as a depth mean and deviation from the mean, $\langle \rangle_z$, and depth variations in u′, s′ are neglected. Then the filtered flux becomes

$$\langle F_h \rangle = \langle h \rangle \langle \bar{u} \rangle \langle \bar{s} \rangle + \langle h'u' \rangle \langle \bar{s} \rangle + \langle \bar{u} \rangle \langle h's' \rangle + \langle h \rangle \langle u's' \rangle + \langle h'u's' \rangle + \overline{\langle u \rangle_z \langle s \rangle_z} \langle h \rangle \tag{12}$$

Due to the sparseness of data points, we cannot venture a definitive statement on the depth-integrated salt flux. Analysis of the terms, however, shows that $\langle \bar{u} \rangle \langle h's' \rangle$ is generally negligible. The remaining terms can all be of the same order, although their relative importance changes during the spring-neap tide cycle. The dominant terms in the equation appear to be $\langle h \rangle \langle \bar{u} \rangle \langle \bar{s} \rangle$ (mean advection of the mean salinity) and $\langle h \rangle \langle u's' \rangle$ (dispersive flux). The net salt flux due to the estuarine circulation $\overline{\langle u \rangle_z \langle s \rangle_z} \langle h \rangle$ is highly variable in both space and time, and is smallest during the spring tides when the water column is well mixed. This flux can be large, however, where the water column stratifies at neap tide.

These same observations hold throughout the northern reach. The data from one current meter array in Suisun Bay show that the net salt flux due to estuarine circulation dominates the salt flux during the period of neap tides.

An examination of mixing in South Bay is hampered by the lack of a suitable tracer as the waters there are isohaline most of the year. During the summer, residual circulation can account for all the mixing in the interior of South Bay. At Bay Bridge (Fig. 1) the residual flow is still an important mixing process, although tidal dispersion can probably be important if there is a suitable difference in salinity between Central and South Bay. During normal to wet winters the density-current exchanges at the northern boundary of South Bay control the exchanges with Central Bay. These density-current exchanges are 3–10 times more important than the summer processes and, hence, promote rapid mixing.

Processes for vertical mixing

Vertical mixing is controlled by the amount of tidal kinetic energy available and by the degree of stratification of the water column. The tidal energy is dependent upon the amplitude of the currents over the spring-neap tidal cycle through the forcing of sea level at Golden Gate, whereas stratification is dependent upon both the mixing intensity and water buoyancy from the freshwater river inflows. Cloern (1984) has related the stratification in South Bay (as represented by the salinity difference between surface and bottom) with a dimensional parameter (Q/u_m^3) where Q is the river inflow and u_m is the tidal-current amplitude. In addition, Haas (1977) has examined the spring-neap variability in salinity for several tributary estuaries of Chesapeake Bay.

We can treat vertical mixing by creating the empirical formulations for the vertical eddy diffusivity

and viscosity and the associated time scales of mixing. We consider two cases: (1) mixing in a homogeneous water column and (2) stratification effects that inhibit mixing. Various mathematical forms for eddy viscosity and diffusivity are given by Bowden & Hamilton (1975) and Kent & Pritchard (1959). For homogeneous conditions, the eddy viscosity, N, varies as

$$N = K_o H u_* (1 - z)z \tag{13}$$

where u_* is friction velocity, K_o is Von Karman's constant, H is depth, and z is a non-dimensional depth (=0 at the bed and =1 at the surface). Following Uncles & Joint (1982), we express u_* in terms of the depth mean velocity u to derive an expression for the maximum value for eddy viscosity,

$$N_{max} = 3 \times 10^{-3}\, Hu \tag{14}$$

and the mean viscosity over the entire water depth,

$$\bar{N} = 2 \times 10^{-3}\, H\bar{u} \tag{15}$$

where $\bar{u}$ is the depth-mean velocity and the overbar denotes a depth average. Finally, we time average this expression over a tidal cycle, yielding the expression

$$<\bar{N}> = 1.3 \times 10^{-3}\, H<\bar{u}>. \tag{16}$$

Assuming that this is equivalent to the eddy diffusivity for homogeneous mixing conditions, we can derive a mixing time scale T for a passive tracer released near the surface (Fischer *et al.*, 1979):

$$T = 0.4\, H^2/<\bar{N}> \quad \text{or} \quad T = 3 \times 10^2\, H/<\bar{u}>. \tag{17}$$

For the shoals adjacent to the Oakland Airport, H = 2 m and $<\bar{u}>$ varies from 12–30 cm s^{-1} over the spring-neap tidal cycle. Then

$$T_{neap} = 1.4 \text{ h}$$
$$T_{spring} = 0.6 \text{ h}. \tag{18}$$

These time scales are probably similar to those of the shoals of San Pablo and Suisun Bays because these shallow areas have similar parameter values. We can repeat this calculation for the deep channels. However, from the results of the tidal analysis, the tidal velocity and hence the RMS tidal velocity varies proportionately with depth so that the change in mixing time scale is somewhat small. For a channel depth of 15 m and a RMS speed of 40 cm s^{-1} (neap) and 70 cm s^{-1} (spring), the mixing time scales are

$$T_{neap} = 3.1 \text{ h}$$
$$T_{spring} = 1.8 \text{ h}. \tag{19}$$

In those cases where the river inflow is small or where tidal mixing can overpower water buoyancy effects, the vertical mixing time scales are as small as those calculated above. However, when salinity stratification becomes important, vertical mixing is reduced and the associated time scale becomes much longer. The magnitude of vertical mixing depends upon a balance between the energy flux caused by water buoyancy and the kinetic-energy flux generated by tidal currents. When the former mechanism dominates the water becomes stratified, whereas when the latter dominates the water becomes well-mixed. The ratio between these two energy fluxes is expressed by a non-dimensional parameter called the Richardson number (Turner, 1973). Although there are several formulas which attempt to compute the eddy viscosity and diffusivity as a function of Richardson number and hence stratification (Kent & Pritchard, 1959; Bowden & Hamilton, 1975), the large scatter in the data precludes the development of a definitive formula.

Acknowledging these uncertainties, we estimate the change in depth-averaged vertical eddy viscosity due to stratification as an order of magnitude reduction from the homogeneous values above. These values are for neap tides and a vertical salinity difference of 5‰ in the channel. The corresponding time scale for mixing is then well over a day.

Residence times

Estimating the mean-residence times for a conservative solute (salt) in various subareas of the bay permits us to define the appropriate time scales associated with physical transport mechanisms so they can be used in conjunction with the time scales for nonconservative chemical and biological pro-

cesses.

We calculate residence times from the total volume of solute within a subarea of the estuary divided by the flux of solute through the boundary. For large fluxes and small volumes the residence time is small, whereas for small fluxes and large volumes the residence time is large. These concepts can be expressed mathematically as

$$V\frac{dc}{dt} = F + \sum_{i=1}^{N} S_i \tag{20}$$

where V is the volume of the subarea, c is the mean concentration of the conservative solute in the subarea, t is time, F is the flux through the boundary, and S_i are the sources within the subarea. If we assume that F and S_i are proportional to c (i.e., first-order processes) and the background concentration of the conservative solute is zero, a solution to the equation is

$$c = c_o \exp(-t/\tau) \tag{21}$$

where c_o is the initial concentration at $t = 0$, and

$$\frac{1}{\tau} = \frac{1}{\tau_F} + \sum_{i=1}^{N} \frac{1}{\tau_i}, \quad \tau_F = \frac{Vc}{F}, \quad \tau_i = \frac{Vc}{S_i} \tag{22}$$

where τ_i are the time scales for the source terms, and τ_F is the time scale for the physical transport processes. Thus, the processes with the shortest time scales have the largest effect upon τ. Because we are only concerned with τ_F, we set $S_i = 0$.

The most straightforward measure of total residence time is the freshwater replacement time where the appropriate volume is the freshwater fraction of the volume of the subarea under consideration and the flux is the river inflow (Conomos, 1979). The residence times for the various embayments are calculated and listed in Table 2. Using a high river inflow of 10^4 m^3 s^{-1} and a low flow of 10^2 m^3 s^{-1}, the residence times for the waters of the northern reach are of the order of days for high river inflows, and months for low inflows. For South Bay the river inflows are primarily through Coyote Creek and Guadalupe River in the south and along the eastcentral portion near Oakland Airport. Here, using high flows of 80 and 20 m^3 s^{-1}, respectively, and low flows of 5 and 3 m^3 s^{-1}, respectively, the residence times are fairly long (i.e. order of several months) during most of the year. We conclude that these measures of residence time for South Bay waters are not appropriate for the observed changes in salinity in the winter and, thus, we must consider exchanges through the northern boundary.

The total residence time above can be broken into its various components. One of these is the hydraulic replacement time, where the applicable volume is the total volume of the subarea under consideration and the flux is that of the freshwater inflow. The hydraulic replacement time is, essen-

Table 2. Calculated residence times, in days, for water masses in various San Francisco Bay embayments. Subarea water-mass volumes and freshwater fractions taken from unpublished data of D. D. Harmon, P. V. Cascos and R. E. Smith. High- and low-flow values for freshwater-fraction calculations are 10^4 and 10^2 m^3 s^{-1}, respectively for the embayments of the northern reach. For South Bay, high-flow values of 80 m^3 s^{-1} and low flows of 5 m^3 s^{-1} are used for Coyote Creek and Guadalupe River discharges; high-flow values of 20 m^3 s^{-1} and low flows of 3 m^3 s^{-1} are used for the minor streams discharging along the east-central shoreline.

Embayment	Sum of all processes		Differentiated processes			
	Freshwater fraction		Hydraulic replacement		Estuarine circulation (vertical)	Residual circulations (horizontal)
	High flow	Low flow	High flow	Low flow		
Suisun Bay	0.5	35	0.5	45	150	150
San Pablo Bay	0.8	25	0.8	84	87	58
Northern reach	1.2	60	1.6	160	240	160
South Bay						
Total	120	160	220	2700	months (summer)	
To Dumbarton Br.	80	120	150	2000	3 days to 2 weeks (winter)	
Below Dumbarton Br.	40	70	75	1200		

tially, the time it takes to replace the water volume of the subarea. The values for the various embayments are listed in Table 2. For the northern reach during high inflow (usually winter), the residence time is dominated by hydraulic replacement, whereas for low flow periods (usually summer) hydraulic replacement accounts for a small portion of the total water residence time and other mechanisms (such as dispersion and estuarine circulation) become more important. Similar results were reported by Glenne (1966) who calculated residence time per unit length of the estuary based on the presence of two processes – hydraulic replacement and dispersion (all remaining processes).

Because of the paucity of data, it is difficult to define the relative importance of the physical transport processes other than hydraulic replacement. Adequate data could allow us to define these processes by time-averaging and cross-sectionally averaging the salt flux where the various terms in the expansion then correspond to the different physical mechanisms (see Dyer, 1974). The available data lead us to suggest that the salt flux at a point (i.e., at a current-meter station) depends mainly on the mean advection of the mean-salt field and on a lesser contribution from tidal dispersion (the correlation between tidal-period salinity and water current). During neap tides when stratification is present, the salt flux due to the estuarine circulation can dominate these terms (Walters & Gartner, 1985). Thus both the net transverse circulation and the net vertical circulation are of importance. The net transverse circulation is identified with 'pumping' and the net vertical circulation with the estuarine circulation. Using the Hansen & Rattray (1966) classification scheme, approximately 30–40% of the upstream salt flux in the northern reach is due to the estuarine circulation and the remainder due to all other processes, probably primarily tidal 'pumping' (Conomos, 1979). Assuming a contribution of 40 and 60% for these two processes, we have calculated the respective residence times necessary to reduce the hydraulic replacement time (defined above) to the freshwater fraction replacement time (i.e. an approximation to the residence time for all physical transport processes).

It is difficult to determine the residence time of the waters of South Bay. The calculated values for freshwater fraction replacement and hydraulic replacement are much larger than the salinity field data suggest. The time scales of salinity changes, from days to weeks in a wet winter to months in the summer, become progressively longer when traveling in a north to south direction. These facts dictate that we consider exchanges between South and Central Bay to properly characterize residence times in South Bay.

Because there is negligible net transfer of water between the two basins for periods of several days or longer, we need only consider those processes involving cross-sectional correlations between currents and salinity rather than mean-advection terms. The residence time of any particular solute will depend upon the details of its spatial distribution across the cross-section between Central and South Bay. Because South Bay is isohaline in summer, the calculations of residence time based on salt distributions then reduce to a hydraulic residence time which is long. Using the calculated bulk diffusivities described by Fischer (1978) from his physical model experiments, we calculate a residence time of about 2 weeks for South Bay. This value seems to have serious uncertainties as it seems intuitively too short by a factor of about five.

When we consider the winter conditions, the data lead us to suggest that South Bay responds rapidly to significant reductions in salinity in Central Bay. For this case where there is a large, transient salinity difference at the north end of South Bay, a density current flows out of South Bay and brackish water flows in. Using the analysis of Dyer (1974, Equation 10, term 7), we calculate a residence time of 3 days for the waters at the northern end of South Bay. When high-salinity water occupies Central Bay and a density current carries saline water into South Bay, the calculated residence time is about 2 weeks. Furthermore, the spring-neap variation in tides as well as the salinity gradient controls the magnitude of the density currents (Figs. 12, 14). Neap tides with pronounced salinity gradients lead to the minimum residence times.

Future research needs

One of a number of gaps in our knowledge of physical processes is an understanding of the currents in the extensive shoal areas. A combination of shallow depths (<2 m), tidal range (2 m) and wind

waves (>1 m) have prevented us from measuring currents there. Additionally, the seasonal variation in the estuarine currents in the northern reach cannot be specified because of the paucity of data.

Our knowledge of processes controlling the flux of solutes is also very limited. Detailed measurements of velocity and salinity over several key cross-sections (i.e. Golden Gate, the northern boundary of South Bay, San Pablo Strait, and Carquinez Strait) are needed. Measurements during typical winter and summer periods will permit us to determine the relative importance of the several physical processes controlling the salt flux and intrusion of saline water into the upper estuary.

Finally, we need to investigate more fully the salt flux over San Bruno and Pinole Shoals by making suitable measurements of velocity and salinity in these areas.

Having created a framework for circulation and mixing, we must attempt to integrate the diverse physical and biological space and time scales present in the estuarine system. Much greater detail is needed in the specification of the water circulation than is needed for biological variables. We are presently interested in the general nature of chemical and biological distributions over large areas. Of importance is the transport between these large areas and the mixing characteristics within them. These mixing rates are then derived from a spatial average of the circulation to derive exchange rates among the various areas. For instance, the exchange rates in the main channel of South Bay are determined by the residual flows – flows that are intimately connected to the variations in bottom topography and that exhibit similar length scales. Since the channel is usually considered homogeneous from a plankton biology perspective, then we must average over the smaller scales of the circulation.

Furthermore, we can hopefully use circulation patterns to identify closed circulation patterns (gyres, etc.) and biologically homogeneous areas. The existence of these areas provides an aid to both the sampling program and to modeling efforts. For instance, there appears to be convergence area in the shoals east of San Bruno Shoal where the biological consequences (i.e. seasonal cycles of chlorophyll concentrations) are profound (Cloern *et al.*, 1985).

References

Bowden, K. F. & P. Hamilton, 1975. Some experiments with a numerical model of circulation and mixing in a tidal estuary. Estuar. coast. mar. Sci. 3: 281–301.

Budgell, W. P., 1982. Spring-neap variation in the vertical stratification of Chesterfield Inlet, Hudson Bay. Naturaliste Can. (Rev. Ecol. Syst.) 109: 709–718.

Cameron, W. M. & D. W. Pritchard, 1963. Estuaries. In M. N. Hill, ed., The Sea, 2. Interscience, N.Y.: 306–324.

Cheng, R. T. & J. W. Gartner, 1984. Tides, tidal and residual currents in San Francisco Bay, California-Results of measurements 1979–1980, Part I through Part V. U.S. Geological Survey Water Resources Investigations Rep 84-4339: 1737 pp.

Cheng, R. T. & J. W. Gartner, 1985. Harmonic analysis of tides and tidal currents in South San Francisco Bay, California. Estuar. coast. shelf Sci. (in press).

Churgin, J. & S. J. Halminski, 1974. Key to oceanographic research documentation, no. 2, Temperature, salinity, oxygen and phosphate in waters off the United States. Eastern North Pacific, National Oceanic and Atmospheric Administration, U.S. Dept. Commerce, Wash., D.C. 3: 259 pp.

Cloern, J. E., 1984. Temporal dynamics and ecological significance of salinity stratification in an estuary (South San Francisco Bay, USA). Oceanol. Acta 7: 137–141.

Cloern, J. E., B. E. Cole, R. L. J. Wong & A. E. Alpine, 1985. Temporal dynamics of estuarine phytoplankton: A case study of San Francisco Bay. Hydrobiologia (this volume).

Conomos, T. J., 1979. Properties and circulation of San Francisco Bay waters. In T. J. Conomos (ed.), San Francisco Bay: The Urbanized Estuary, Pacific Division, Am. Ass. Adv. Sci., San Francisco, Calif.: 47–84.

Conomos, T. J., R. E. Smith, D. H. Peterson, S. W. Hager & L. E. Schemel, 1979. Processes affecting seasonal distributions of water properties in the San Francisco Bay estuarine system. In T. J. Conomos (ed.), San Francisco Bay: The Urbanized Estuary. Pacific Division, Am. Ass. Adv. Sci., San Francisco, Calif.: 115–141.

Conomos, T. J., R. E. Smith & J. W. Gartner, 1985. Environmental setting of San Francisco Bay. Hydrobiologia (this volume).

Darwin, G. H., 1962. The tides and kindred phenomena in the solar system. W. H. Freeman & Co., San Francisco, Calif.: 378 pp.

Disney, L. P. & W. H. Overshiner, 1925. Tides and currents in San Francisco Bay. U.S. Dept. Comm., U.S. Coast and Geodetic Survey, Spec. Pub. 115: 125 pp.

Dyer, K. R., 1974. The salt balance in stratified estuaries. Estuar. coast. mar. Sci. 2: 273–281.

Fischer, H. B., 1978. Flushing of South San Francisco Bay, Rep. HBF-78/01: Hugo B. Fischer, Inc., Berkeley, Calif.: 103 pp.

Fischer, H. B. & E. Dudley, 1975. Salinity intrusion mechanism and San Francisco Bay, California. Proc. 16th Congr. Int. Ass. Hydraulic Res. 1: 124–133.

Fischer, H. B., E. J. List, R. C. Y. Koh, J. Imberger & N. H. Brooks, 1979. Mixing in inland and coastal waters. Academic Press, N.Y., 483 pp.

Gilbert, G. K., 1917. Hydraulic-mining debris in the Sierra

Nevada. U.S. Geological Survey Prof. Paper 105: 154 pp.
Glenne, B., 1966. Diffusive processes in estuaries. Univ. of Calif. (Berkeley) Sanitary Engineering Research Laboratory Rep. 66-6: 78 pp.
Haas, L. W., 1977. The effect of the spring-neap tidal cycle on the vertical salinity structure of the James, York and Rappahannock River, Virginia, U.S.A. Estuar. coast. mar. Sci. 5: 485–496.
Hansen, D. V. & M. Rattray, Jr., 1966. New dimension in estuary classification: Limnol. Oceanogr. 11: 319–326.
Hughes, F. W. & M. Rattray, Jr., 1980. Salt flux and mixing in the Columbia River estuary. Estuar. coast. mar. Sci. 10: 479–493.
Imberger, J., W. B. Kirkland, Jr. & H. B. Fischer, 1977. The effect of delta outflow on density stratification in San Francisco Bay. Assoc. Bay Area Gov. Rep. HBF-77/02. Berkeley, Calif.: 109 pp.
Kent, R. E. & D. W. Pritchard, 1959. A test of mixing length theories in a coastal plain estuary. J. mar. Res. 18: 62–72.
Kirkland, W. B. Jr. & H. B. Fischer, 1976. Hydraulic model studies (San Francisco Bay-Delta model) for East Bay Dischargers Authority. March 31, 1976. Water Front Associates, Alameda, Calif.: 44 pp.
McCulloch, D. S., D. H. Peterson, P. R. Carlson & T. J. Conomos, 1970. Some effects of fresh-water inflow on the flushing of south San Francisco Bay: A preliminary report. U.S. Geological Survey Circular 637A: 27 pp.
National Oceanic and Atmospheric Administration, 1979. Tidal current tables 1980. Pacific Coast of North America and Asia. NOAA, U.S. Dept. Commerce, Washington, D.C.: 260 pp.
Officer, C. B., 1976. Physical oceanography of estuaries (and associated coastal waters). Wiley & Sons, New York: 465 pp.
Orlob, G. T., 1977. Impact of upstream storage and diversions on salinity balance in estuaries. M. Wiley (ed.) Estuarine Processes. 2. Academic Press, New York: 3–17.
Peterson, D. H., 1979. Sources and sinks of biologically reactive oxygen, carbon, nitrogen, and silica in northern San Francisco Bay. In T. J. Conomos, (ed.), San Francisco Bay: The Urbanized Estuary. Pacific Div. Am. Ass. Adv. Sci., San Francisco, Calif.: 175–193.
Peterson, D. H., T. J. Conomos, W. W. Broenkow & P. C. Doherty, 1975. Location of the non-tidal current null zone in northern San Francisco Bay. Estuar. coast. mar. Sci. 3: 1–11.
Peterson, D. H., R. E. Smith, S. W. Hager, D. D. Harmon & L. E. Schemel, 1985. Interannual variability in dissolved inorganic nutrients in northern San Francisco Bay estuary. Hydrobiologia (this volume).
Schureman, Paul, 1940. Manual of harmonic analysis and prediction of tides: (reprinted with corrections 1976), U.S. Coast and Geodetic Survey, Special Publication 98, 317 pp.
Tee, K.-T., 1977. Tide-induced residual current – verification of a numerical model. J. Phys. Oceanogr. 7: 396–401.
Turner, J. S., 1973. Buoyance effects in fluids. Cambridge University Press, Cambridge, 368 pp.
Uncles, R. J., 1982. Computed and observed residual currents in the Bristol Channel. Oceanol. Acta 5: 11–20.
Uncles, R. J. & I. R. Joint, 1982. Vertical mixing and its effects upon phytoplankton growth in a turbid estuary. Can. J. Aquat. Sci. 4, supp. 1: 221–228.
Walters, R. A., 1982. Low frequency relations in sea level currents in South San Francisco Bay. J. Phys. Oceanogr. 12: 658–668.
Walters, R. A. & R. T. Cheng, 1980. Calculations of estuarine residual currents using the finite element method. In D. H. Norrie (ed.), Proc. 3rd Int. Conf. Finite Elements in Flow Problems. U. of Calgary: 60–69.
Walters, R. A. & C. Heston, 1982. Removing tidal period variations from time-series of water surface elevations using low-pass digital filters. J. Phys. Oceanogr. 12: 112–115.
Walters, R. A. & J. W. Gartner, 1985. Subtidal sea level and current variations in the northern reach of San Francisco Bay. Estuar. coast. shelf Sci. (in press).